ISSN 1748-3182

BIOINSPIRATION & BIOMIMETICS

Learning from nature

Volume 3 Number 2 June 2008

bb.iop.org

IOP Publishing

IOP PUBLISHING BIOINSPIRATION & BIOMIMETICS

Bioinsp. Biomim. **3** (2008) 026002 (11pp) doi:10.1088/1748-3182/3/2/026002

A robotic device for understanding neuromechanical interactions during standing balance control

J E Scrivens[1], S P DeWeerth[2] and L H Ting[2,3]

[1] Department of Mechanical Engineering, Interdisciplinary Bioengineering Program, Georgia Institute of Technology, 313 Ferst Drive, Atlanta, GA 30332-0535, USA
[2] Department of Biomedical Engineering, Georgia Institute of Technology and Emory University, 313 Ferst Drive, Atlanta, GA 30332-0535, USA

E-mail: lting@emory.edu

Received 31 November 2007
Accepted for publication 20 March 2008
Published 25 April 2008
Online at stacks.iop.org/BB/3/026002

Abstract

Postural stability in standing balance results from the mechanics of body dynamics as well as active neural feedback control processes. Even when an animal or human has multiple legs on the ground, active neural regulation of balance is required. When the postural configuration, or stance, changes, such as when the feet are placed further apart, the mechanical stability of the organism changes, but the degree to which this alters the demands on neural feedback control for postural stability is unknown. We developed a robotic system that mimics the neuromechanical postural control system of a cat in response to lateral perturbations. This simple robotic system allows us to study the interactions between various parameters that contribute to postural stability and cannot be independently varied in biological systems. The robot is a 'planar', two-legged device that maintains compliant balance control in a variety of stance widths when subject to perturbations of the support surface, and in this sense reveals principles of lateral balance control that are also applicable to bipeds. Here we demonstrate that independent variations in either stance width or delayed neural feedback gains can have profound and often surprisingly detrimental effects on the postural stability of the system. Moreover, we show through experimentation and analysis that changing stance width alters fundamental mechanical relationships important in standing balance control and requires a coordinated adjustment of delayed feedback control to maintain postural stability.

(Some figures in this article are in colour only in the electronic version)

1. Introduction

When considering medial–lateral balance control, people generally experience increased stability and ease of control when they increase the distance between the feet, or stance width. For example, people often widen their stance when standing on a moving train to avoid falling. Presumably, the medial–lateral stability of the body increases with a wider stance. Accordingly, when stance width is increased, muscle activation levels are shown to decrease in response to translational perturbations of the support surface in the horizontal plane (Torres-Oviedo *et al* 2006, Henry *et al* 2001). These observations demonstrate the dependence of the overall system behavior on both configuration-dependent musculoskeletal mechanics and the active muscular responses evoked by a perturbation through neural feedback control (Dunbar *et al* 1986, Horak and Macpherson 1996).

However, the specific contributions and interactions between the mechanical and neural systems to postural response behaviors are not well understood. The decreased muscle responses at wide stance widths suggest that the

[3] Address for correspondence: The W H Coulter Department of Biomedical Engineering, Emory University and Georgia Institute of Technology, 313 Ferst Drive Atlanta, GA 30332-0535, USA.

magnitude of active neural feedback control decreases, but it is not clear how these changes are quantitatively related to configuration-dependent changes in the dynamics of the musculoskeletal system. Intuitively, mechanical stability increases with stance width, but do the associated neural-control requirements also change? Since these factors co-vary during normal postural behaviors, it is difficult to study the independent contributions of the neural and mechanical systems to postural behaviors in an animal system.

We are interested explicitly in the contributions of and interactions between neural feedback control and mechanical dynamics during standing balance. Postural stability results from both the active neural responses of the postural controller and the mechanical dynamics of the musculoskeletal system. We hypothesize that, in order to maintain postural stability, changes in either musculoskeletal mechanics or neural feedback control necessitates concurrent changes in the other. We developed a simple robotic system to explicitly decouple these neuromechanical interactions that naturally occur in an organism, allowing us to characterize and quantify the neuromechanical relationships that give rise to postural stability. The system was developed to mimic the motion of a cat subjected to lateral-displacement perturbations to the support surface (Macpherson 1988b). Changes to the mechanical dynamics were induced by changing the stance width of the robot. Changes to delayed neural feedback control gains were introduced through the real-time control of the motor torques.

The system design was based on established models of postural dynamics and control in *frontal-plane* (medio-lateral) motion (Day *et al* 1993, Gage *et al* 2004, Prince *et al* 1995, Rietdyk *et al* 1999, Winter *et al* 1996). The robot's two legs can represent frontal-plane motion in bipedal humans as well as quadrupedal cats. In simulations of frontal-plane postural control, abduction and adduction torques applied at the hips have been shown to generate corrective responses to postural perturbations (Winter *et al* 1996). To mimic these responses, we implemented a delayed neural feedback controller similar to those previously used to describe postural control in both humans and animals (Lockhart and Ting 2007, Ishida *et al* 1997, Kuo 1995, Kiemel *et al* 2002, Park *et al* 2004, van der Kooij *et al* 1999). Corrective hip-joint torques were generated in proportion to hip-joint displacement and velocity. We implemented two parallel feedback loops: one with a long-latency time delay to mimic neural feedback control from sensory inputs, and the other with zero delay to mimic the instantaneous effects of the intrinsic properties of muscle and connective tissue (Peterka 2002). While current models of standing posture range in complexity from the most detailed models, which take into account multiple sensory systems including visual, vestibular, proprioceptive and tactile inputs (Jo and Massaquoi 2004, van der Kooij *et al* 1999, Peterka 2002), we used a simple sensory input model with a single feedback loop (Barin 1989, Morasso and Schieppati 1999, Rietdyk *et al* 1999, Park *et al* 2004).

In this paper, we first describe the design, function and initial testing of the robot to evaluate its utility in studying standing balance. We then detail our investigation and analysis of the neuromechanical interactions between stance width and feedback gains in the control of standing balance and determine a function describing the necessary interactions between stance width and delayed feedback gains to maintain postural stability.

2. System design

The robot, *Floppy*, was designed to mimic the motion of a cat subjected to lateral perturbation and enables postural stability to be altered through modulation feedback gains, stance width and intrinsic muscle properties. We first describe the physical system design, including robot mechanics and the test platform used to deliver support-surface perturbations. We then describe the real-time control implementation and algorithms used to generate the simulated neural feedback responses, the intrinsic muscle stiffness, as well as compensation for non-physiological characteristics of the robotic implementation. These characteristics include friction and transmission losses in the motor and drive train.

2.1. Robot mechanics

The robot is a three-segment device with a rigid lumped mass equivalent to that of a cat torso and two rigid legs (figure 1(*A*)). Stance width can be varied by placing the robot on a flat surface with the legs at different angles. When the feet remain in contact with the ground and do not slip, the resulting configuration is a four-bar linkage. Each of the two hip joints has one rotational degree of freedom and is independently driven by a coreless dc micromotor (Faulhaber 2342-024CR) through a timing belt and pulley (SDP-SI MXL) with a 12:1 drive ratio (figure 1(*B*)). Although the direct drive of each leg would minimize transmission losses and rotational inertia, this design would be impractical, requiring a larger motor, which would not fit within the desired design envelope and which would be damaged by the desired 90° working angle of the leg. The selected transmission system adds minimal weight, provides high transmission efficiency through a one-stage design and enables the use of the smaller motor that operates through multiple revolutions.

The robot was designed to have size and weight characteristics similar to a cat. The distance between the hip joints and the height of the robot were sized to match the pelvis width and leg length of a small house cat. Structural components were designed to minimize the mass. However, additional brass components were added to give the system a final mass of 2 kg, about half the weight of a standard cat and representing either the front or rear portion of the cat. To give the robot stability in the sagittal plane and to provide room to house the motors inside the body, the legs were designed with a depth of 65 mm (figure 1(*B*)).

As a freestanding device, the robot is unrestrained and the feet are free to slip or 'step' under perturbation. To provide friction and model the compliance of the foot–ground contact, the ends of the legs were covered with silicone foam

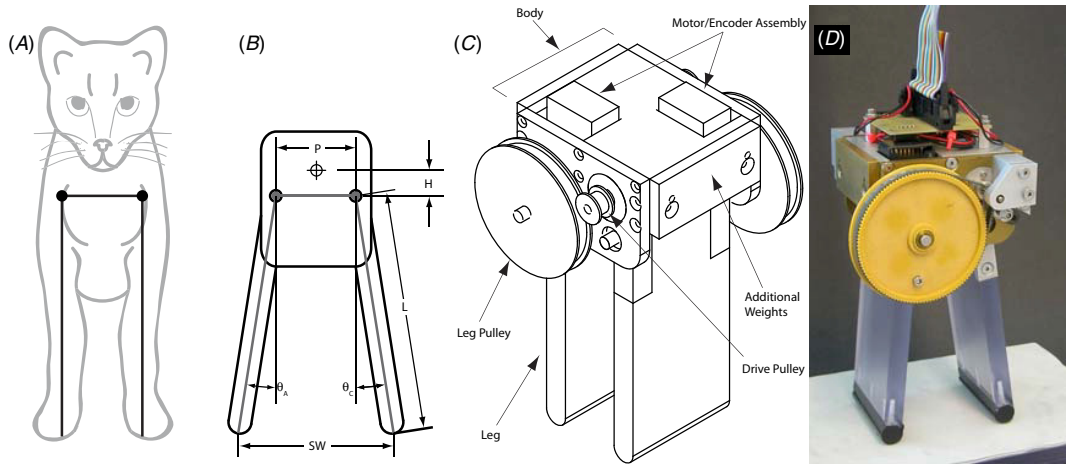

Figure 1. *Floppy* robot design. (*A*) The motion of a cat subjected to a lateral displacement perturbation is modeled by the motion of a four-bar linkage. (*B*) This motion is replicated by a three-segment device representing a rigid lumped torso and independently controlled legs. Basic parameters of the system are detailed in table 1. (*C*) To implement a device with this mechanical configuration, we designed a robot with a torso and two legs that are independently driven by coreless dc motors through a timing belt/pulley transmission system. Using this transmission system enabled the production of the required torque from small motors while maintaining the low mechanical impedance that facilitates 'floppy' legs. Position feedback for each hip joint is obtained via rotary encoders coupled to the motors. Additional weights were added to achieve cat dimensions. The final version of *Floppy* is shown in frame D.

Table 1. Mechanical properties

Symbol	Quantity	Value
P	Hip width	4.4 cm
H	CoM position	1.9 cm
θ_A, θ_B, θ_C	Stance angle	0–30°
SW	Stance width	4.4–8.9 cm
L	Leg length	14 cm
M	Mass	2 kg
I_T	Torso inertia	2.19×10^{-3} kg m^2
I_L	Leg inertia	3.38×10^{-4} kg m^2

(McMaster-Carr 86235K132). Like cat paws, this compliance provides a small amount of shear compliance (>1 mm) and absorbs some of the impact of a step, eliminating bounce and aiding in the maintenance of traction. The surface of the platform was also covered with a 1.6 mm layer of silicone rubber (McMaster-Carr 86465K34) to increase friction between the feet and the support surface. The final implementation of *Floppy* is shown in figures 1(*C*) and (*D*), and the model dimensions and inertias are shown and listed in figure 1 and table 1, respectively.

To maintain the simplicity of the system and to avoid the requirement of onboard computation and energy storage, the robot is electrically interfaced to a host computer through custom interface boards and a single suspended ribbon cable. The ribbon cable minimally affects the dynamics of the robot response. This interface cable provides current to the motors and joint-position feedback to the controller. Joint position is measured using an optical rotary encoder attached directly to the motor. Working through the drive transmission, the encoders give a final joint resolution of 0.007 radians. The drive motor for each leg is controlled by a PWM current driver (Advanced Motion Controls Z6A6DDC). The current drivers are used because the objective of the controller is to specify the torque applied to each joint, and in dc motor operation, torque is proportional to current.

2.2. Robot control

The controller we use has two feedback processes: a delayed *active* loop to simulate neural processing and control, and a non-delayed *intrinsic* component to simulate activation-dependent muscle properties (Ishida *et al* 1997, Kuo 1995, Kiemel *et al* 2002, Park *et al* 2004, van der Kooij *et al* 1999). The long-latency active component of the response is modeled as a feedback loop of joint acceleration, position and velocity, with a lumped time delay that models the neural transmission and processing delays associated with postural responses to perturbation (Welch and Ting 2008, Lockhart and Ting 2007, Horak and Macpherson 1996). Feedback control utilizing hip angular displacement, velocity and acceleration is used to generate corrective hip-joint torques (figure 2). The instantaneous intrinsic component of the feedback loop is modeled as a variable viscoelastic component at the joint (figure 2), representing the mechanical properties of a muscle with a stretch-reflex response, which has been shown to enhance the muscle stiffness at timescales shorter than the postural response delay (Nichols and Houk 1976, Huyghues-Despointes *et al* 2003a, 2003b). The viscoelastic components are variable parameters because the elastic modulus of a muscle varies with the muscle tension (Joyce and Rack 1969, Huyghues-Despointes *et al* 2003a) and can be voluntarily regulated by changing muscle activation patterns (Bunderson *et al* 2008, Hogan 1984). With the active and intrinsic components acting independently, the postural controller is similar to the parallel cascade model of postural response (Kearney *et al* 1997, Mirbagheri *et al* 2000).

To minimize the effects of viscous mechanical losses in the robotic mechanisms, we also implemented a feedback

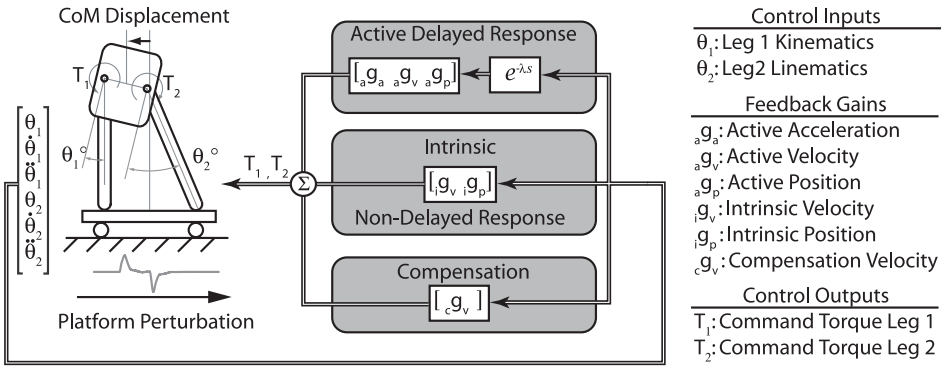

Figure 2. Feedback control schematic. To achieve independently variable active and intrinsic responses, we used parallel feedback loops. The intrinsic response can be described as an instantaneous linear pathway with elastic and viscous properties due to muscle and reflex properties. The active response can be described as a delayed pathway with elastic, viscous and inertial elements. A third feedback compensation component was added to compensate for the mechanical losses of the drive system.

compensation loop that operated in parallel to the active and intrinsic feedback loop (figure 2). This control component is a positive feedback gain term that was tuned experimentally to reduce damping in the free-swinging leg. This compensation helps ensure that the dynamic responses of the system are not simple artifacts of the dynamics of the motor and transmission. For example, when the compensation system is not active, the motors themselves have enough friction and damping to stabilize leg motion without any need for feedback control. With a compensation term in the feedback loop (figure 2), the legs of the robot are compliant, or 'floppy', like a biological system, thus giving rise to its name, and it requires feedback control to stand up and to maintain balance following perturbations.

The postural controller was implemented using a Simulink™ (MathWorks Inc.) model running on a dSPACE DS1103 real-time processor running at 5 kHz (dSPACE Inc.). A custom MATLAB user interface allows the feedback gains to be varied in the robot, controls the perturbation delivered by the platform (described below) and allows automated data collection for parameter variation studies.

2.3. Platform

We developed a motion platform to apply the lateral support-surface perturbations similar to those used in human and cat experiments (Macpherson *et al* 1987, Torres-Oviedo *et al* 2006, Horak *et al* 2005, Henry *et al* 1998, Brown *et al* 2001). We created a single-axis motion platform that delivers velocity step perturbations for a specified distance. The displacement platform is a 25 × 15 cm surface. The platform rides on two linear rails and four Rulon™-coated linear bearings and is driven by two dc micro-motors with a custom PWM motor driver in velocity mode through a 9.7 mm pitch diameter pulley and a timing belt. The system is capable of accelerating the robot mass at 600 cm s^{-2} with a peak velocity of more than 100 cm s^{-1} and a maximum platform displacement magnitude of 32 cm. Platform control is implemented as an independent component of the Simulink™ model. Its control is not directly tied to the control of the robot except for the shared computational resources. The platform is operated under high gain PID feedback control.

3. Validation

To validate the robot as a model of standing balance, we compared the motion of the robot subjected to a lateral displacement perturbation to the motion of a cat subjected to a similar perturbation. We also evaluated the efficacy of our of feedback compensation by comparing the motion of the robot to the dynamics of a simulation. The computational model was based on the physical parameters of the device. The equations of motion were developed in Autolev™ and the simulations were run in the C programming environment. The results of these simulations assisted in the evaluation of responses over the range of control experimental parameters.

To find the nominal feedback gains for our robot and mimic the postural response of the cat, we compared the robot's responses to perturbation to those of a cat. To make this comparison, we first replicated the stance of and the perturbation applied to the cat. We then empirically tuned the feedback gains until the kinematic response of the robot resembled the kinematic response of the cat. The perturbation magnitude and the responses of the cat were obtained from previously performed lateral perturbation trials (Macpherson 1988a, 1994). The perturbations had a velocity and magnitude of 15 cm s^{-1} for 4.0 cm, respectively.

After validating the system, we conducted a series of tests to demonstrate that the dynamic characteristics of the postural response to perturbation could be dramatically altered by changes in the control parameters (feedback gain and delay) as well as changes in mechanical configuration (stance width). These results demonstrate that biologically relevant, compliant postural stability cannot be solely attributed to either the feedback controller or mechanical configuration alone.

We demonstrated the dependence of the postural response on both stance and feedback gain parameters by applying lateral perturbations to the standing robot while independently varying stance width and feedback gains. In each series of trials the postural performance of the system was compared

to its performance while using a reference set of variables. The perturbations of the 20 cm s^{-1} displacement magnitude for a 100 ms duration were applied. These perturbations were challenging enough to make the system fall if a response was inappropriate.

The response of the robot was evaluated by measuring the motion of the center of mass (CoM) following perturbation. The robot is a one-degree-of-freedom system and the motion of the CoM represents the overall dynamic response of the system. However, the CoM position is not a directly measured variable. Instead, because of the geometric constraints of the system, the stance width (SW) and CoM displacement relative to the perturbation platform (X_{CoM}) are calculated from the independent leg angles (θ_1 and θ_2), leg length (L), pelvis width (P) and vertical position of the CoM (H):

$$\begin{aligned} \Delta x &= P + L\sin(\theta_1) + L\sin(\theta_2) \\ \Delta y &= L\cos(\theta_1) - L\cos(\theta_2) \\ SW &= \sqrt{\Delta x^2 + \Delta y^2} \\ X_{\mathrm{CoM}} &= P\cos(\theta_2) + L\sin(\theta_1 - \theta_2) - \tfrac{SW}{2} - H\sin(\theta_2). \end{aligned} \tag{1}$$

4. Results

Results from our validation tests show that the compensated robot is capable of mimicking the response of a cat and exhibiting a range of responses through variation of either stance width or feedback gain. This section details the results of each of the validation procedures listed in section 3. These results include calibration of the compensation parameter, mimicry of the cat response, descriptions of the dynamic effects and interactions between stance width and feedback gain variations.

4.1. System calibration

As described in section 2.2, the compensation feedback loop reduced the effects of viscous damping due to the motor and belt transmission of the robot. When mounted horizontally to negate the influence of gravity on the motion of the leg, leg velocity decreases steadily when given an initial angular velocity, coming to rest or reaching the limit of rotation (figure 3(*A*), dashed lines). After compensation, the leg maintained the near-constant angular velocity throughout the full range of motion (figure 3(*A*), solid lines). Careful consideration was taken to obtain a parameter that minimized velocity loss for both legs without any increase in velocity, which might destabilize the system. In the final tuning, the compensation parameter was established with the coefficient of 0.004 N m s rad^{-1}.

The performance of the robot and the effects of compensation on response dynamics were further evaluated by comparing the response kinematics of the robot to the response kinematics resulting from an idealized, frictionless simulation. Under most conditions, the compensation does not greatly alter the response of the system (figure 3(*B*)), and the simulated and robot responses are similar with or without compensation. However, under certain test conditions where the simulation oscillated unstably, only the robot with feedback compensation

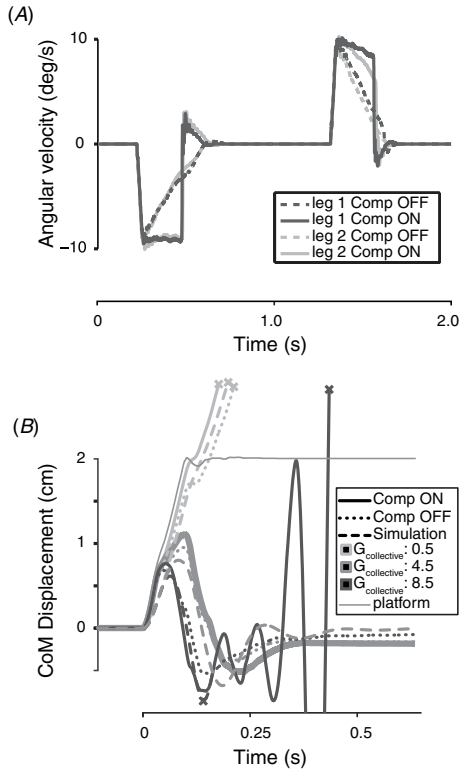

Figure 3. Validation of feedback compensation and comparison of robot response to simulation. (*A*) When given an initial angular velocity, the uncompensated and unloaded leg has a rapidly declining angular velocity (dashed lines). Feedback compensation adds a positive velocity feedback to counteract mechanical damping in the system so that leg velocity is maintained (solid lines). (*B*) Robot responses, with and without compensation, and simulation results all have similar kinematics (dark lines). However, without compensation, robot responses may display stable behavior when simulation results and compensated responses are unstable.

was unstable, whereas the response without compensation was stable with damped oscillation (figure 3(*B*), dark traces). These results indicate that without compensation, the motors provide a non-physiological source of stability. Another benefit of having a quantifiable measure of compensation is that it provides a reasonable estimate of the difference between the simulation and the robot characteristics.

We identified four types of responses to postural perturbation, which could all be achieved through independent variation of either stance width or feedback gains (figure 4). The *unstable insufficient* response occurs when the robot does not return toward the center position and falls over as a result of the perturbation (figure 4(*A*)). The *stable damped* response is the most ideal response, enabling a quick recovery from the perturbation with a critically damped or over-damped response (figure 4(*B*)). The *stable oscillatory* response also generates a sufficient response to recover from the perturbation, but has an under-damped behavior with a short period of oscillation (figure 4(*C*)). In an *unstable oscillatory* response, the system persistently overshoots the center position in its recovery attempt, resulting in oscillations that increase in magnitude until the system falls over or

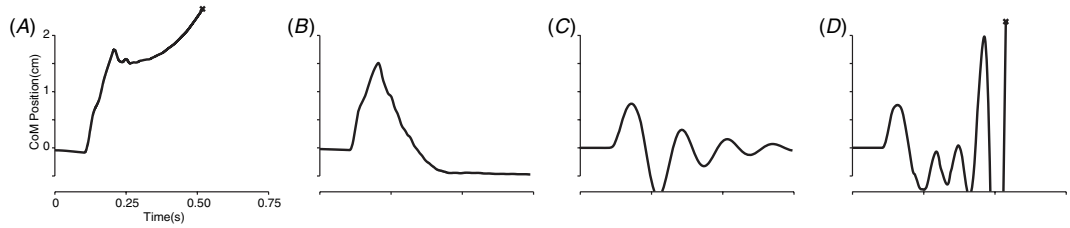

Figure 4. Typical CoM position response types. (*A*) Insufficient feedback gain results in an unstable response in which insufficient torque is generated and the robot falls over. (*B*) When feedback gains are appropriate for the current stance width, the system exhibits a stable response that recovers from the perturbation. The stable response can be critically damped or over-damped. (*C*) The stable response can also be under-damped resulting in decreasing oscillations. (*D*) Excessive gain results in an unstable response that oscillates with increasing amplitude until the leg limits are reached, the system jumps off of the table and the trial is stopped.

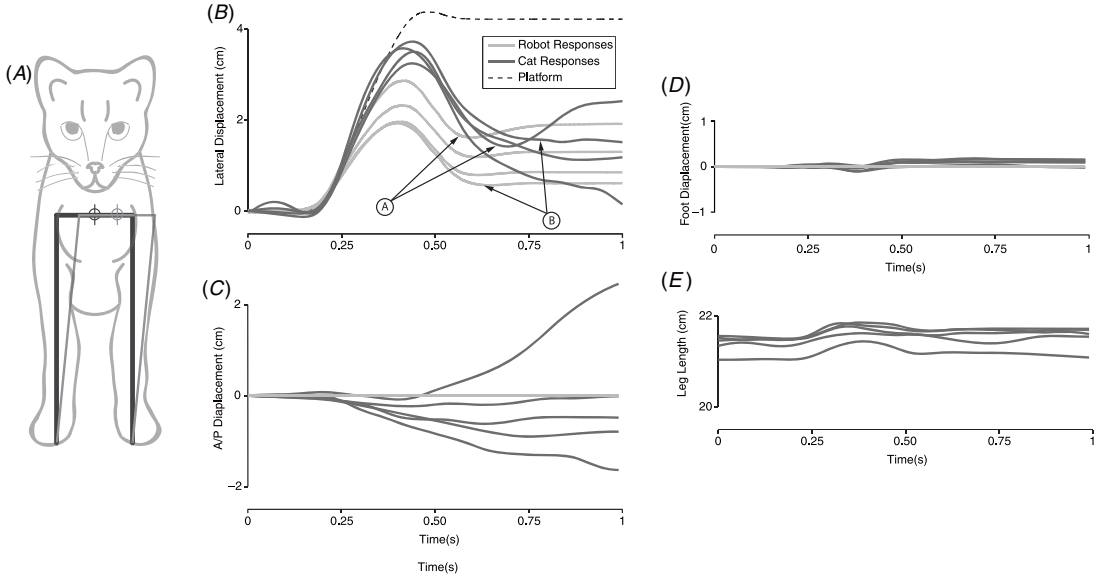

Figure 5. Experimentally measured response to lateral displacement perturbation in a cat compared to robot responses. (*A*) When subjected to lateral displacement perturbation, the response of a cat is a planar movement equivalent to that of a four-bar linkage. (*B*) Lateral displacement of the center of mass (CoM) is highly correlated to the perturbation, and both the cat and the robot in preferred stance exhibit kinematic responses that overshoot and do not return to the original center position. (*C*) Anterior/posterior displacement in the cat is not related to the perturbation. Also, consistent with the four-bar linkage model, (*D*) the feet of the cat do not move and (*E*) the legs maintain a constant length throughout the perturbation response.

jumps off the platform (figure 4(*D*)). These responses can be described in control terminology as negatively damped (positive velocity feedback).

4.2. Mimicking the cat response

The kinematics of a cat subjected to lateral displacement perturbations of the support surface can be modeled as a four-bar linkage (figure 5(*A*)). Experimental data (Torres-Oviedo *et al* 2006) demonstrate that CoM motion is primarily in the frontal plane and closely follows the medial–lateral (M/L) perturbation (figure 5(*B*)). Motions in the anterior–posterior (A/P) direction may occur later in the trial, but are unrelated to the perturbation direction (figure 5(*C*)). Consistent with a four-bar linkage model, the foot displacement is minimal and the overall limb length is relatively constant throughout the postural response (figures 5(*D*) and (*E*)). Moreover, the anterior and posterior portions of the cat's body displace together during lateral perturbations; therefore, the motion of a single pair of limbs can represent the response of the entire body, making it equivalent to a biped.

Using various combinations of active and intrinsic feedback gains, we were able to mimic the dynamic response of a cat subjected to displacement perturbation (figure 5(*B*)). The robot was set at a 3° stance angle to match the preferred stance of the cats and then subjected to a perturbation similar to the one used in the cats. The robot mimicked the dynamic qualities of the cat's motion using gain magnitudes that ranged from 0.4 to 0.6 N m rad^{-1} and 0.04 to 0.06 N m s rad^{-1} for the position and velocity feedback, respectively, and intrinsic gain magnitudes of 0.05 N m rad^{-1} and 0.005 N m s rad^{-1}. The results of these trials show that both the cat and the robot responses can be described as a damped motion without a return to the center starting position. The results further show that the cat and the robot generate a range of responses that may smoothly approach a final position or overshoot the final position before coming to rest following the perturbation.

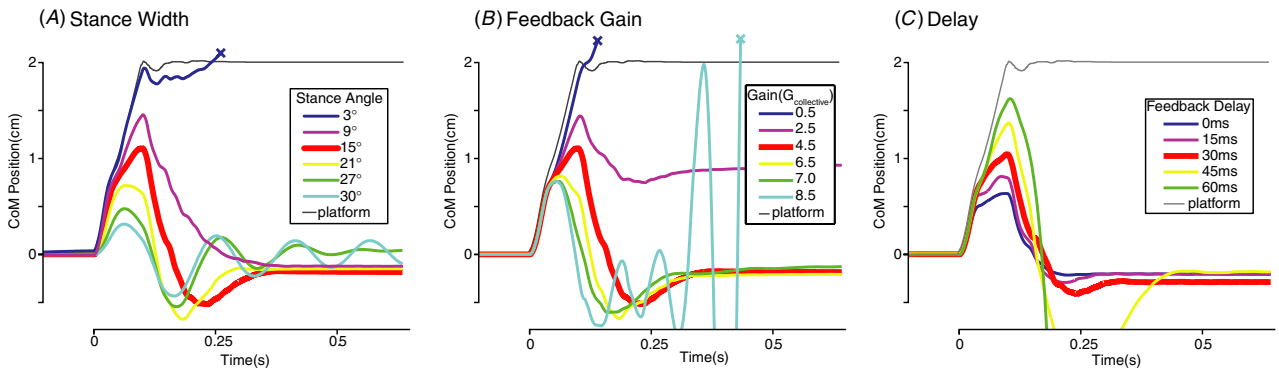

Figure 6. Variation of response dynamics with changing parameters. (*A*) Increasing stance width decreases the magnitude of the initial displacement. However the increasing stance width also increases the oscillations of the response indicating that the system may be approaching the limits of stability before exhibiting wild oscillations. (*B*) A uniform increase in feedback gains increases the speed of the postural response. This is shown by a faster return toward the center position and increased oscillations. The increasing gain also decreases the magnitude of the initial excursion. However, the decrease in the initial excursion is limited and eventually reaches a minimum excursion magnitude. (*C*) Feedback delay has a destabilizing effect on the dynamics of the system. With an increased delay, the initial excursion increases and the responses develop more overshoot during their return to the center. As the delay is further increased, the responses eventually become unstable.

Table 2. Nominal response parameters

Variable	Value
Stance angle	15°
Velocity feedback gain	0.045 N m s rad^{-1}
Position feedback gain	0.450 N m rad^{-1}
Feedback delay	30 ms

4.3. Dynamic effects of varying delayed feedback control and stance width

To evaluate the change in response dynamics that occurs with variations of stance width and feedback gain, we established a nominal response to perturbation and assessed the change relative to the nominal response. The parameters for the nominal response were selected to represent the 'middle of all parameters' and are listed in table 2. The kinematic response arising from this nominal set of parameters is shown as the thick trace in the center of each trial series shown in figure 6.

Increasing the stance width while holding the feedback gains constant at the nominal values resulted in a stiffer, more oscillatory system (figure 6(*A*)). Peak CoM excursion decreased linearly with increased stance width, which might be interpreted as increased stability. However, response oscillations also increased with stance width indicating that the system may be on the verge of instability. As the stance width was reduced, the initial displacement increased and the oscillations in the response decreased. At the narrowest stance of 3°, the robot did not return toward the center position and fell over as a result of perturbation (figure 6(*A*), blue trace). These results suggest that variations of stance width do not simply alter the magnitude of the response, but they affect the dynamic characteristics of the response as well.

The variations of responses that we observed under changing stance widths were also observed under changing magnitudes of the feedback gain. The feedback gains are the control variables that are used in the generation of the torque responses to perturbations (figure 2). We varied displacement and velocity feedback gains ($_{a}g_{p}$ and $_{a}g_{v}$) as functions of a single scaling parameter ($G_{\text{collective}}$). Scaling gains by this single parameter maintained a constant 10:1 ratio between displacement and velocity feedback. As $G_{\text{collective}}$ was increased, the speed of the postural responses increased, with a faster return to the center position (figure 6(*B*)). These responses were similar to the ones observed under increasing stance width. As the feedback gain was increased from a low magnitude, responses became stronger with faster returns to the center position and increasing oscillations. As with the responses under varying stance width, the robot does not return toward the center position and falls over under the lowest gain and oscillates wildly and falls over under the highest gain.

A major difference between the varying stance width responses and the varying gain responses was that increasing gain did not reduce the initial excursion magnitude as much as the increasing stance width (figures 6(*A*) and (*B*)). However, we observed that for both series of trials (stance width variation and gain variation), an inflection point consistently occurred at $t \approx 30$ ms. We hypothesized that the magnitude of the excursion may be more influenced by the feedback delay than by the magnitude of the gains. Therefore, we also examined the effects of varying the duration of the feedback delay on postural performance.

We found that the delay has a destabilizing effect on the postural response and may limit the range of the stable gain magnitude observed in the earlier trials (figure 6(*C*)). With no feedback delay, the system exhibits a stable over damped response (figure 8(*A*), blue trace). As the feedback delay was increased, initial excursion increased and the system became less damped with increasing overshoot in the response (figure 6(*C*)). With a feedback delay of 45 ms, the response overshoot increased and had a magnitude that was approximately equal to the peak initial displacement. With a feedback delay of 60 ms, the system had the highest peak initial displacement magnitude and became rapidly unstable.

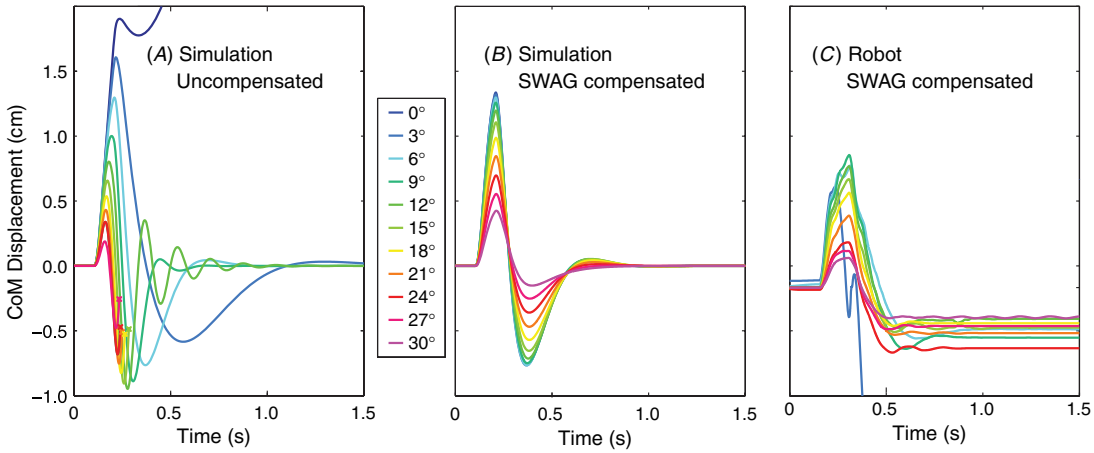

Figure 7. Postural response dynamics in simulations and the robot. (*A*) Variation of stance width under constant feedback gain results in slower responses in narrow stances and faster responses in wide stances. (*B*) Simulated implementation of the SWAG function, which adjusts the feedback gains to maintain similar postural response dynamics results in consistent postural responses across stances. Despite the difference in the initial displacement magnitudes between the stances, oscillation frequencies and settling times are all the same. (*C*) Implementation of the SWAG function on the robot also results in similar perturbation responses across stance widths.

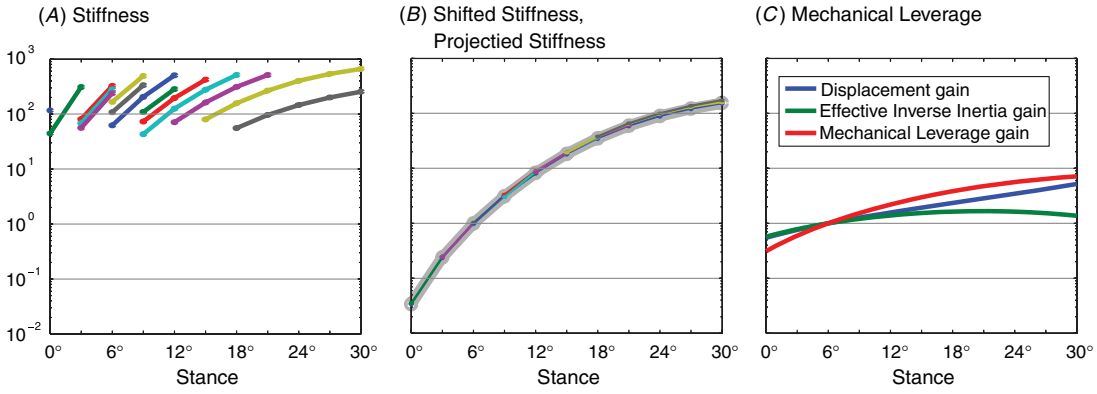

Figure 8. (*A*) Evaluation of postural response trends shows that response stiffness increases with increasing stance width. Close inspection of the stiffness trends also shows that the stiffness increase (slope) is stance change dependent and feedback gain independent. (*B*) Shifting the individual stiffness curves reveals the gain-independent change in stiffness that occurs across the stance range. This stiffness curve is also calculated by averaging the independent slopes and extrapolating a single curve from those averages (gray curve). (*C*) Evaluating the mechanical system we determined that two important mechanical relations change under the stance width variation, effective inertia and the displacement ratio between the leg angle and CoM displacement. These two relations combine as the mechanical leverage variation of stance width changes.

4.4. Interactions between delayed feedback control and stance width for postural control

Because postural response dynamics varied so dramatically when stance width was varied, but feedback gains were held constant, we sought to derive a function by which the delayed feedback gains should be modulated as a function of stance width to produce consistent postural control over a wide range of stance widths. To this end, we derived the stance width adjustment of gain (SWAG) function, which allows us to identify important characteristics of the system contributing to changing postural stability at different stance widths. We then applied the function to the robot to test its efficacy in modulating feedback gains to maintain a consistent postural response at a range of stance widths.

In order to derive the SWAG function, we first quantified the effective stiffness of the overall postural response dynamics of the simulated system at a range of stance widths and feedback gains by fitting the CoM displacement trajectory to a second-order system. In simulations, as in the robot, the same delayed feedback gains applied to different stance widths cause a wide variation in postural response dynamics (figure 7(*A*)). Under constant feedback gains, the effective stiffness of the postural responses increased with increased stance width (figure 8(*A*), solid lines). Because each stance width required different feedback gains for stability, each feedback gain was tested across few configurations where stable responses were achieved (figure 8(*A*), each colored line represents the constant gain). Thus, at each configuration, multiple feedback gains were also tested.

We then generated a curve that demonstrates the change in effective stiffness that would occur with variations in stance width if a single set of gains could produce stable responses across the full range of stance widths (figure 8(*B*)). At a given stance width, the change in effective stiffness for an increment change in stance width was the same regardless of the feedback gain value (figure 8(*A*), compare slopes). Therefore, the change in stiffness does not depend upon the magnitude of the feedback gains. These constant slopes, or the rate change of stiffness with stance width, were used to project the effects of the stance width variation across the full range of stance widths for a given feedback gain. This projection can be illustrated by shifting each curve in figure 8(*A*) so that the end points lie on top of each other and produce a single curve (figure 8(*B*), multicolor curves). The same result was found by extrapolating effective stiffness based on the average slope at each stance width (figure 8(*B*), grey curve). In each case, the resulting stiffness was normalized by the effective stiffness at a 6° stance.

Mechanical analysis of the four-bar-linkage structure revealed two relationships that are important to the control of standing posture when stance width varies. First, the inverse of the effective inertia determines the magnitude of the hip torque required to produce a desired acceleration of the CoM. As stance width increases, effective inertia decreases and its inverse increases, so the CoM accelerates faster for a given torque applied at the hip (figure 8(*C*), green curve). Secondly, the ratio between the change in the leg angle and change in the CoM displacement affects the amount of hip torque that is applied by the feedback rule for a given perturbation to the CoM. As stance width increases, the more the leg angle changes for a given displacement of the CoM (figure 8(*C*), blue curve). As a result, for the same amplitude of the CoM displacement, greater torques are generated in a wide stance compared to a narrow stance when the same feedback gains are used (figure 8(*C*), blue curve). The overall changes in the effective stiffness of the system due to changing the mechanics of the system, which we call *mechanical leverage gain* (figure 8(*C*), red curve), can be found by multiplying the effects of the effective inverse inertia and the displacement gain. Although the combined effect of these two stance-dependent relationships generates higher hip torques and accelerates the CoM more for a given torque applied in a wide stance compared to a narrow stance, the effects of mechanical leverage alone were insufficient to account for the large increases in stiffness actually measured in our system (compare figures 8(*B*) and (*C*)).

The additional changes in the effective stiffness measured in our system could be accounted for by considering the effects of the time delay in the feedback look in addition to the mechanical leverage gain. The effect of the time delay can be explained through an analogy to a mass–spring–damper system (figure 9(*A*)), where the effective stiffness with no feedback delay matches that predicted through mechanical considerations alone. However, with a 30 ms feedback delay (figure 9(*B*)), the effective stiffness increases to a value greater than that of the mechanical system with no delay and increases in a manner analogous to that in our postural model

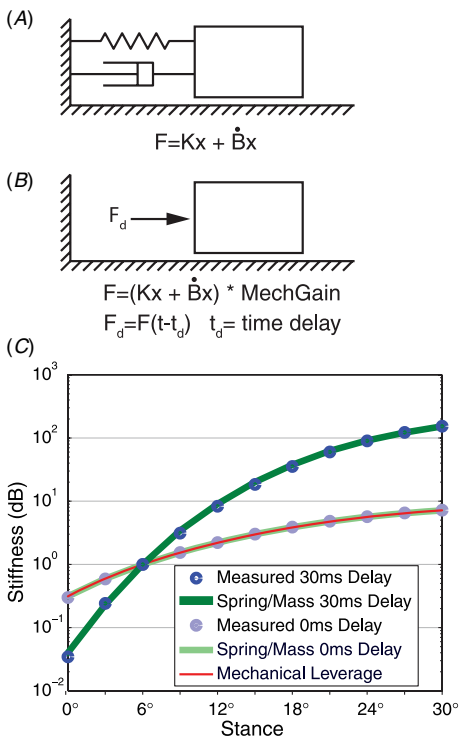

Figure 9. (*A*) The combined effects of the mechanical leverage variation and feedback time delay were evaluated by studying a simple spring–mass–damper system. (*B*) The forces of the spring and damper were replaced by an equivalent forcing function with a time delay. Mechanical leverage was implemented by scaling the magnitude of the forcing function. (*C*) Without feedback delay, the change in the effective stiffness of the response is equivalent to the mechanical leverage shown in figure 8(*C*). However, with a 30 ms feedback delay the change in the effective stiffness exceeds the mechanical leverage and matches the change in stiffness measured in the simulated system.

(figure 9(*C*)). Therefore, the observed increase in stiffness is due to the combined effect of mechanical leverage and the time delay in the feedback loop.

Finally, we needed to consider the variations in the CoM position at a given stance width to compute the SWAG function. The mechanical leverage values shown in figure 9 were computed for initial CoM positions that were centered between the two legs. However, during a perturbation response, the robot does not remain in that position and mechanical leverage varies slightly with lateral displacement from the upright position. Therefore, we used displacement magnitudes of 80% of the maximum possible CoM displacement for each stance width to compute the effects of mechanical leverage gain and delay. From these computations, we generated the SWAG function, which provides a multiplicative factor at each stance width to modify feedback gains so that consistent postural responses can be achieved at all stance widths (figure 10).

When adjusted by the SWAG function, the temporal dynamics of the postural responses were similar across all stance widths, in both the simulation and robot (figures 7(*B*) and (*C*)). When using the SWAG function to adjust gains when

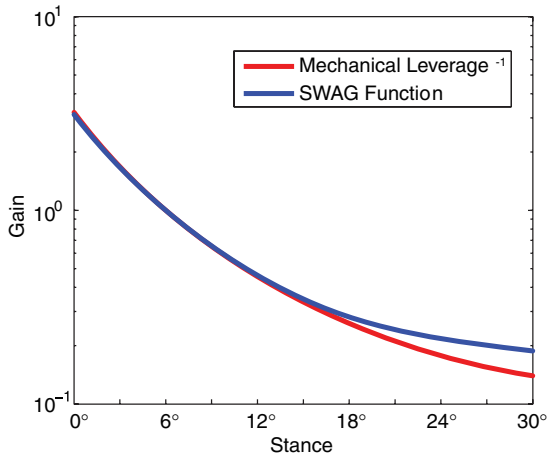

Figure 10. In its final implementation, the SWAG function is similar to the inverse of mechanical leverage; however it is due to the variation of mechanical leverage under displacement in a time-delayed system. This effect is most pronounced in wide stances where mechanical leverage varies considerably under the CoM displacement.

changing stance width, the range of postural responses in the simulation and robot that were highly divergent (figures 6(*A*) and 7(*A*)) had the same oscillation frequency and settling times, although the peak overshoot still varied with stance width. The only exception was in the narrowest stance in which the robot fell over under perturbation (figure 7(*C*)).

5. Discussion

The robotic system, *Floppy*, was developed to study the coordinated contributions of postural mechanics and compliant delayed feedback control to the stability of standing balance. We verified that *Floppy* is capable of generating postural responses that closely resemble the responses of a cat. Surprisingly, modulating the feedback gain or stance configuration can invoke similar alterations in the dynamic system response in a delayed-feedback system for balance control. For example, increasing stance width while holding the feedback gain constant has the effect of increasing the stiffness of the system as shown by faster responses with more oscillations. Similarly, independently increasing feedback gain at a given stance width also increases the stiffness of the system resulting in faster, more oscillatory responses. The similarity of these effects on system stiffness suggests that the dynamics of the postural response are linked to both parameters and that performance characteristics can be maintained through coordinated alteration of both parameters.

Our results demonstrate that achieving consistent postural response dynamics is dependent on coordinating the delayed feedback gains to the standing postural configuration. This linked effect emphasizes importance of coordinated co-modulation of stance width and feedback gain for postural stability. Furthermore we show that changes in stance width can be coordinated with a change in feedback gains according to our SWAG function, to produce in a system that has similar dynamic responses across different stance widths. The SWAG function has direct implications to the implementation of robotic systems in which postural control is desired, facilitating the modification of feedback gains as a function of stance width. Additionally, our analyses have demonstrated regions of instability—which must be avoided in such implementations—that results from certain combinations of gain and stance width, which are amplified by the presence of feedback delays.

The results of this study may provide insight into the results of previous studies in biological systems where mechanics and feedback control gains appear to co-vary. For example, our results support the experimental findings that increased stance width in humans and cats results in postural responses with the consistent CoM displacement but decreased muscle activity (Torres-Oviedo *et al* 2006, Henry *et al* 2001). The decreased muscle response was originally attributed to an increase in intrinsic stiffness of the musculoskeletal system. However, our results suggest that the decreased CoM displacement should occur at wider stance widths if the feedback control is constant. The prior experimental result may be explained by a decrease in neural feedback gains at wide stance widths without any need for changing the intrinsic muscle properties.

We acknowledge that directly relating these results to the results of animal and human studies must be done carefully. There are a number of differences that distinguish this system from physiological systems. Furthermore certain modeling assumptions were made in the design of this system including the use of gain magnitudes based on metric variables and the use of lumped torso mass. Since the system uses gains based on engineering terms, the gain magnitudes of the device will not correlate with physiological gains. However, our studies and physiological studies primarily examine the scaling of gains with physical parameters and responses. Therefore, gain changes of this robotic system may parallel gain changes in physiological systems. Also, this system has a single rigid body mass as a torso and hip. This configuration is in contrast with the human torso, which can flex and arc laterally. However, the rigid configuration is commonly used in models of a lateral standing posture (Full and Koditschek 1999, Henry *et al* 1998, Horak *et al* 2005, Winter *et al* 2003, 1996), although a flexible spine model has also been used (Rietdyk *et al* 1999).

Even with these noted differences, this robotic system has a unique ability to address questions about biological control of posture and the interaction of control and mechanical stability. We demonstrated that the mechanical stability, neural feedback control and the interaction between these factors contribute to the overall postural stability in this biomimetic model of a standing posture. The analyses afforded by this device will allow us to more precisely quantify these important interactions. Ultimately, the knowledge gained in this and future studies will help prove useful as we make advances in rehabilitation, neural prosthetic design and robotics.

Acknowledgments

This robot development project was funded in part by the National Institute of Health (1R01EB00786-01) and by the Center for Behavioral Neuroscience.

References

Barin K 1989 Evaluation of a generalized model of human postural dynamics and control in the sagittal plane *Biol. Cybern.* **61** 37–50

Brown L A, Jensen J L, Korff T and Woollacott M H 2001 The translating platform paradigm: perturbation displacement waveform alters the postural response *Gait Posture* **14** 256–63

Bunderson N E, Burkholder T J and Ting L H 2008 Reduction of neuromuscular redundancy for postural force generation using an intrinsic stability criterion *J. Biomech.* in press doi:10.1016/j.jbiomech.2008.02.004

Day B L, Steiger M J, Thompson P D and Marsden C D 1993 Effect of vision and stance width on human body motion when standing: implications for afferent control of lateral sway *J. Physiol.* **469** 479–99

Dunbar D C, Horak F B, Macpherson J M and Rushmer D S 1986 Neural control of quadrupedal and bipedal stance: implications for the evolution of erect posture *Am. J. Phys. Anthropol.* **69** 93–105

Full R J and Koditschek D E 1999 Templates and anchors: neuromechanical hypotheses of legged locomotion on land *J. Exp. Biol.* **202** 3325–32

Gage W H, Winter D A, Frank J S and Adkin A L 2004 Kinematic and kinetic validity of the inverted pendulum model in quiet standing *Gait Posture* **19** 124–32

Henry S M, Fung J and Horak F B 1998 EMG responses to maintain stance during multidirectional surface translations *J. Neurophysiol.* **80** 1939–50

Henry S M, Fung J and Horak F B 2001 Effect of stance width on multidirectional postural responses *J. Neurophysiol.* **85** 559–70

Hogan N 1984 Adaptive control of mechanical impedance by coactivation of antagonist muscles *IEEE Trans. Autom. Control* **29** 681–690

Horak F B, Dimitrova D and Nutt J G 2005 Direction-specific postural instability in subjects with Parkinson's disease *Exp. Neurol.* **193** 504–21

Horak F B and Macpherson J M 1996 Postural orientation and equilibrium *Handbook of Physiology* section 12 (New York: American Physiological Society)

Huyghues-Despointes C M, Cope T C and Nichols T R 2003a Intrinsic properties and reflex compensation in reinnervated triceps surae muscles of the cat: effect of activation level *J. Neurophysiol.* **90** 1537–46

Huyghues-Despointes C M, Cope T C and Nichols T R 2003b Intrinsic properties and reflex compensation in re-innervated triceps surae muscles of the cat: effect of movement history *J. Neurophysiol.* **90** 1547–55

Ishida A, Imai S and Fukuoka Y 1997 Analysis of the posture control system under fixed and sway-referenced support conditions *IEEE Trans. Biomed. Eng.* **44** 331–6

Jeka J, Kiemel T, Creath R, Horak F and Peterka R 2004 Controlling human upright posture: velocity information is more accurate than position or acceleration *J. Neurophysiol.* **92** 2368–79

Jo S and Massaquoi S G 2004 A model of cerebellum stabilized and scheduled hybrid long-loop control of upright balance *Biol. Cybern.* **91** 188–202

Joyce G C and Rack P M 1969 Isotonic lengthening and shortening movements of cat soleus muscle *J. Physiol.* **204** 475–91

Kearney R E, Stein R B and Parameswaran L 1997 Identification of intrinsic and reflex contributions to human ankle stiffness dynamics *IEEE Trans. Biomed. Eng.* **44** 493–504

Kiemel T, Oie K S and Jeka J J 2002 Multisensory fusion and the stochastic structure of postural sway *Biol. Cybern.* **87** 262–77

Kuo A D 1995 An optimal control model for analyzing human postural balance *IEEE Trans. Biomed. Eng.* **42** 87–101

Lockhart D B and Ting L H 2007 Optimal sensorimotor transformations for balance *Nat. Neurosci.* **10** 1329–36

Macpherson J M 1988a Strategies that simplify the control of quadrupedal stance: I. Forces at the ground *J. Neurophysiol.* **60** 204–17

Macpherson J M 1988b Strategies that simplify the control of quadrupedal stance: II. Electromyographic activity *J. Neurophysiol.* **60** 218–31

Macpherson J M 1994 Changes in a postural strategy with inter-paw distance *J. Neurophysiol.* **71** 931–40

Macpherson J M, Lywood D W and van Eyken A 1987 A system for the analysis of posture and stance in quadrupeds *J. Neurosci. Methods* **20** 73–82

Mirbagheri M M, Barbeau H and Kearney R E 2000 Intrinsic and reflex contributions to human ankle stiffness: variation with activation level and position *Exp. Brain Res.* **135** 423–36

Morasso P G and Schieppati M 1999 Can muscle stiffness alone stabilize upright standing? *J. Neurophysiol.* **82** 1622–6

Nichols T R and Houk J C 1976 Improvement in linearity and regulation of stiffness that results from actions of stretch reflex *J. Neurophysiol.* **39** 119–42

Park S, Horak F B and Kuo A D 2004 Postural feedback responses scale with biomechanical constraints in human standing *Exp. Brain. Res.* **154** 417–27

Peterka R J 2002 Sensorimotor integration in human postural control *J. Neurophysiol.* **88** 1097–118

Prince F, Winter D A and Archer S E 1995 Assessment of postural control during quiet stance with different foot configurations *Gait Posture.* **3** 110

Rietdyk S, Patla A E, Winter D A, Ishac M G and Little C E 1999 NACOB presentation CSB New Investigator Award. Balance recovery from medio-lateral perturbations of the upper body during standing. *North American Congress on Biomechanics J. Biomech.* **32** 1149–58

Torres-Oviedo G, Macpherson J M and Ting L H 2006 Muscle synergy organization is robust across a variety of postural perturbations *J. Neurophysiol.* **96** 1530–46

van der Kooij H, Jacobs R, Koopman B and Grootenboer H 1999 A multisensory integration model of human stance control *Biol. Cybern.* **80** 299–308

Welch T D and Ting L H 2008 A feedback model predicts muscle activity during human postural responses to support surface translations *J. Neurophysiol.* **99** 1032–8

Winter D A, Patla A E, Ishac M and Gage W H 2003 Motor mechanisms of balance during quiet standing *J. Electromyogr. Kinesiol.* **13** 49–56

Winter D A, Prince F, Frank J S, Powell C and Zabjek K F 1996 Unified theory regarding A/P and M/L balance in quiet stance *J. Neurophysiol.* **75** 2334–43